CONF-9010185--2

DE91 001493

Potential Impact of Enhanced Fracture-Toughness Data on Pressurized-Thermal-Shock Analysis

T. L. Dickson and T. J. Theiss

Engineering Technology Division
Oak Ridge National Laboratory
Oak Ridge, Tennessee

To be presented at the **18th Water Reactor Safety Information Meeting**
Holiday Inn Crowne Plaza Hotel,
Rockville, Maryland
October 22-24, 1990.

Potential Impact of Enhanced Fracture-Toughness Data on Pressurized-Thermal-Shock Analysis*

T. L. Dickson and T. J. Theiss
Engineering Technology Division
Oak Ridge National Laboratory
Oak Ridge, Tennessee

Abstract

The Heavy Section Steel Technology (HSST) Program is involved with the generation of "enhanced" fracture-initiation toughness and fracture-arrest toughness data of prototypic nuclear reactor vessel steels. These two sets of data are enhanced because they have distinguishing characteristics that could potentially impact PWR pressure vessel integrity assessments for the pressurized-thermal shock (PTS) loading condition which is a major plant-life extension issue to be confronted in the 1990's.

Over the past several years, the HSST Program at Oak Ridge National Laboratory (ORNL) has performed a series of large-scale fracture- mechanics experiments. These experiments have produced crack-arrest (K_{Ia}) data with the distinguishing characteristic that the values are considerably above 220 MPa • $\sqrt{m}$, the implicit limit of the ASME Code and the limit used in the Integrated Pressurized Thermal Shock (IPTS) studies. Currently, the HSST Program is planning experiments to verify and quantify, for A533B steel, the distinguishing characteristic of elevated initiation-fracture toughness for shallow flaws which has been observed for other steels.

Deterministic and probabilistic fracture-mechanics analyses were performed to examine the influence of the enhanced initiation and arrest fracture- toughness data on the cleavage fracture response of a nuclear reactor pressure vessel subjected to PTS loading. The results of the analyses indicated that application of the enhanced K_{Ia} data does reduce the conditional probability of failure P(F|E); however, it does not appear to have the potential to significantly impact the results of PTS analyses. The application of enhanced fracture-initiation-toughness data for shallow flaws also reduces P(F|E), but it does appear to have a potential for significantly affecting the results of PTS analyses.

The effect of including Type I warm prestress in probabilistic fracture-mechanics analyses is beneficial. The benefit is transient dependent and, in some cases, can be quite significant.

Introduction and Background

During the early 1970's, it was recognized that reactor pressure vessels could be subjected to severe thermal shock as the result of a large-break loss-of-coolant accident (LBLOCA). Analyses

*Research sponsored by the Office of Nuclear Regulatory Research, U.S. Nuclear Regulatory Commission under Interagency Agreement 1886-8011-9B with the U.S. Department of Energy under Contract DE-AC05-84OR21400 with Martin Marietta Energy Systems, Inc.

performed at that time indicated that thermal shock alone would not result in failure (through-wall cracking) of the vessel. However, a combination of pressure and a less severe thermal shock, the result of some postulated transients, could result in vessel failure. In March 1978, such a transient occurred at the Rancho Seco nuclear power plant. As a result of these events, parametric pressurized-thermal shock (PTS) studies were undertaken [1]. These studies indicated a rather high probability of vessel failure for PTS-loading conditions occurring at the end of the licensing period; as a result, in May 1981, the Nuclear Regulatory Commission (NRC) established the Integrated Pressurized-Thermal-Shock (IPTS) Program. An objective of that program was to estimate the probability of vessel failure caused by through-wall cracking. The results of the IPTS Program [2,3,4] along with risk assessments and fracture analyses performed by the NRC and reactor system vendors, led to the establishment of the NRC PTS rule (10 CFR 50.61), which includes screening criteria in the form of limiting values of the reference nil-ductility transition temperature (RT_{NDT}) of the reactor vessel [5]. The PTS rule required that plant-specific analyses be performed for any plant that is intended to operate beyond the screening criteria. In addition, Regulatory Guide 1.154 [6] provides guidance for utilities on how to perform the plant-specific safety analyses. It references the IPTS study as an acceptable methodology for performing the probabilistic fracture-mechanics portion of the plant-specific analysis.

Since the IPTS Program was completed, the Heavy Section Steel Technology (HSST) Program has conducted several large-specimen fracture-mechanics experiments. In these experiments, it was demonstrated that prototypic reactor vessel steels are capable of arresting a propagating crack at values of fracture toughness considerably above 220 MPa • $\sqrt{m}$, the implicit limit of the American Society of Mechanical Engineers (ASME) code [7] and the limit included in the IPTS studies [8].

Recent research at the University of Kansas [9,10] has shown that the initiation-fracture toughness measured using shallow-crack specimens is significantly elevated over the plane-strain fracture toughness in materials whose stress-strain properties bracket those of A533B steel, a prototypical nuclear reactor pressure vessel steel. Conventionally, the fracture-initiation toughness of a material is determined using specimens in which the crack depth is approximately one-half the depth of the specimen (a/w = 0.5). This eliminates the influence of the specimen boundaries on the crack-tip region as much as possible and provides a plane-strain value for fracture toughness. The shallow crack enhanced initiation toughness is of interest since the relative number of undetected flaws in a vessel wall is large for shallow-crack depths and the IPTS study used the same plane-strain fracture-toughness curve as a basis to determine initiation for all flaws [2, 3, 4]. It is anticipated that A533B steel will demonstrate a similar effect for shallow flaws; therefore, the HSST Program is currently planning experiments to verify and quantify this distinguishing characteristic for A533B steel [11].

It is anticipated that some plants will exceed the PTS-screening criteria during this decade. Pressure vessel integrity has been identified as the major issue confronting the NRC on Plant Life Extension; therefore, evaluating the influence of enhanced fracture- toughness data on the results of IPTS-type probabilistic fracture-mechanics analyses is appropriate and timely. The purpose of this paper is to investigate the potential impact of the enhanced initiation and arrest fracture-toughness data on the results of deterministic and probabilistic fracture-mechanics analyses.

Effect of Enhanced K_{Ia} Data on Deterministic Fracture-Mechanics Analyses

The large-scale crack-arrest experiments conducted by the HSST Program demonstrated that crack-arrest values exist well above the ASME implicit limit of 220 MPa • $\sqrt{m}$ for prototypical nuclear reactor pressure vessel steels [12,13,14,15]. Figure 1 shows how the contributions from the large

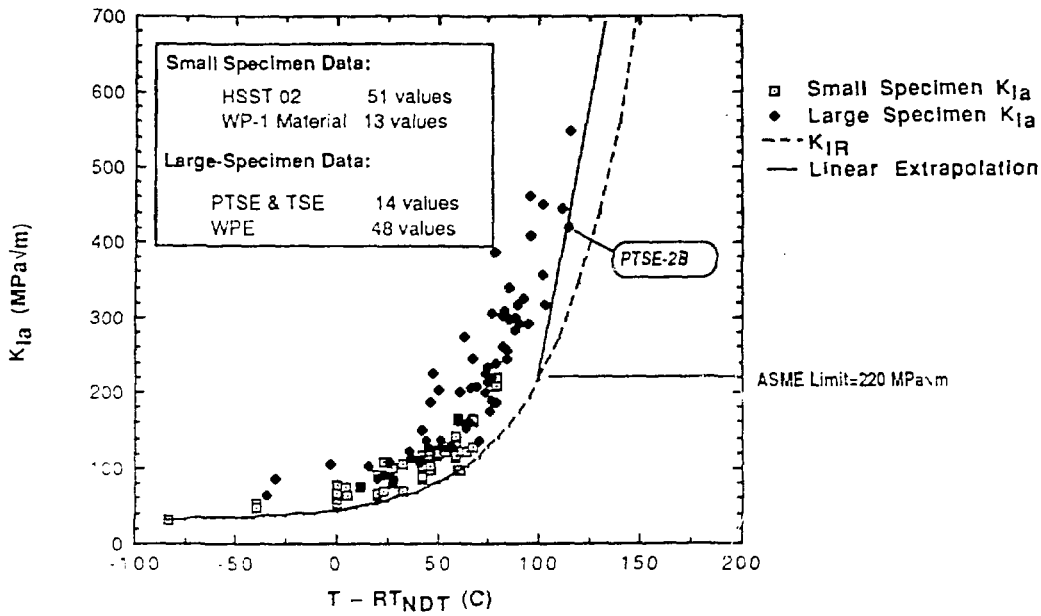

Fig. 1. Combined large- and small-specimen HSST K_{Ia} data base (two extrapolations above 220 MPa • $\sqrt{m}$).

specimen HSST crack-arrest tests have expanded the HSST crack-arrest data base. In all large-specimen experiments, the crack propagated by cleavage to the point of arrest. For the large specimens, most of the arrest events were followed by cleavage reinitiation or unstable ductile tearing. It should be noted that the HSST wide-plate experiment K_{Ia}-data points shown in Fig. 1 have been adjusted (reduced by 20%) to account for tunneling.

Figure 1 also shows two extrapolations above the ASME implicit limit of 220 MPa • $\sqrt{m}$. As can be seen from Fig. 1, the extrapolation of the ASME lower-bound K_{Ia} curve (K_{IR} curve) does not take advantage of the increasing steepness suggested by the data. The straight-line extrapolation of the ASME curve above 220 MPa • $\sqrt{m}$, fitted through the limiting point (from experiment PTSE-2B), is a more accurate lower bound of the data. This is in keeping with the ASME spirit of using a lower-bound curve which is not transgressed by any of the data points.

Deterministic fracture-mechanics analyses were performed to examine the influence of the large-specimen K_{Ia} data on the cleavage fracture response of a nuclear reactor pressure vessel subjected to a PTS-loading scenario. Analyses were performed using OCA-P [16], a program developed at Oak Ridge National Laboratory specifically for simulating the fracture response of a reactor vessel subjected to a PTS event. The cleavage fracture response of the Rancho Seco PTS event was predicted using both of the extrapolated K_{Ia} curves shown in Fig. 1. The Rancho Seco transient was chosen because it is reasonably typical of a postulated, higher-pressure "dominant" transient. Also, previous analyses, using the ASME K_{IR} curve truncated at 220 MPa • $\sqrt{m}$, had predicted failure of the vessel at the end of the licensing period. The pressure and thermal transients for Rancho Seco are shown in Fig. 2 [16].

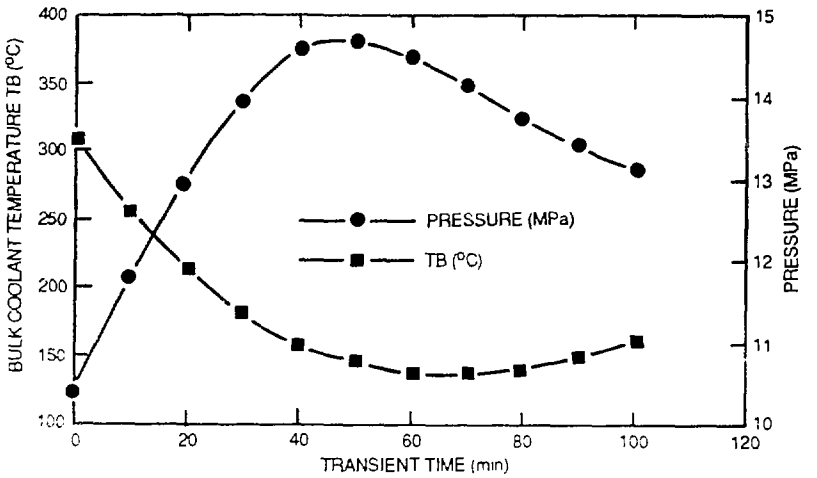

Fig. 2. Pressure and temperature time histories based on idealization of Rancho Seco transient.

The critical crack-depth arrest curves (the locus of points in the crack-depth transient-time plane for which $K_I = K_{Ia}$) corresponding to both extrapolated K_{Ia} curves (shown in Fig 1) are shown in Fig 3. Also, the definition of "cleavage-initiation window" is illustrated in Fig 3 to be the time period and range of crack depths for which a cleavage crack initiation can occur. The cleavage-initiation window is a function of the K_{Ic} curve, the value of RT_{NDT}, and the location of the warm-

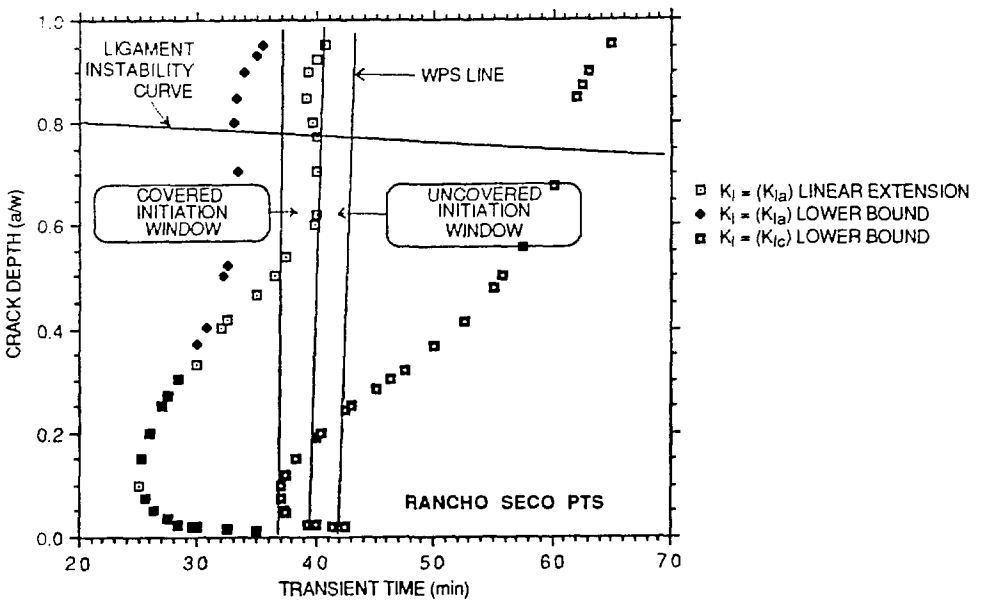

Fig. 3. K_{Ia} linear extrapolation showing reduction of range of flaw depths that can result in failure.

prestress (WPS) line which is transient dependent. Crack initiation and reinitiation do not occur for times greater than those corresponding to the WPS line because $\dot{K}_I < 0$ [13,14,15]. The critical crack-depth arrest curves were generated assuming a fast neutron fluence (E > 1.0 MeV) of 1.5 x 10^{19} neutrons/cm^2 which corresponds to 32 EFPY; copper and nickel concentrations of 0.35% and 0,65%, respectively; and two-dimensional, axially oriented surface flaws. Also, the critical crack-depth initiation curve (the locus of points in the crack-depth transient time plane for which $K_I=K_{Ic}$) was generated using the lower-bound ASME-K_{Ic} curve.

The critical crack-depth arrest curve corresponding to the extrapolated ASME-K_{IR} curve (shown in Fig. 3) does not "cover" any part of the cleavage-initiation window; therefore, any crack initiation occurring in the initiation window is predicted to propagate through the vessel wall thickness, resulting in failure.

To evaluate the effect of the steeper linear extrapolated lower-bound K_{Ia} curve, the following crack-arrest criteria was incorporated into the OCA-P code:

$$K_{Ia} = K_{IR} \text{ (ASME Equation)} \qquad \text{for } K_{Ia} < 220 \text{ MPa} \cdot \sqrt{m}$$

$$K_{Ia} = 15.0 \text{ X } (T\text{-}RT_{NDT}) - 1300. \qquad \text{for } K_{Ia} > 220 \text{ MPa} \cdot \sqrt{m}$$

As illustrated in Fig. 3, the critical crack-depth arrest curve corresponding to the steeper K_{Ia} extrapolation does cover part of the initiation window which increases the chances of crack arrest. The effect of the steeper K_{Ia} curve is to reduce the range of flaw depths that can result in failure. In principle, the steeper K_{Ia} curve should decrease the conditional probability of failure calculated in a probabilistic fracture-mechanics analysis. The degree to which it does so is examined in more detail later in this paper.

Ductile Tearing Considerations

As illustrated above, the application of the large-specimen K_{Ia} data results in an enhanced crack-arrest potential. Many of the large-specimen crack-arrest events that occurred at values of $K_I >$ 220 MPa $\cdot \sqrt{m}$ were followed immediately by a fracture-mode conversion to unstable ductile tearing leading to failure [12, 13, 14]. It is possible that the onset of unstable ductile tearing could negate the benefit of the enhanced crack-arrest potential; therefore, unstable ductile tearing must be considered before making the generalization that the enhanced crack-arrest potential decreases the probability of failure.

To determine if unstable ductile tearing negates the enhanced crack arrest potential, a curve was generated on the critical crack-depth plot that approximates the onset of unstable ductile tearing, that is, the crack depth at which ductile tearing becomes unstable. The associated critical crack depths correspond to the point of tangency between the tearing-resistance curve (J_R) and applied load (J applied) curves, in which case the point of tangency represents the initial flaw depth value plus extension due to tearing up to the point of instability [17].

A graphical solution was used to find the point of tangency between the curves for various times throughout the transient. An example in Figure 4 shows the point of tangency between the Japplied curve at time=3000 sec for the Rancho Seco PTS event and the average J_R curve for a temperature of 288°C. The point of tangency defines the initial crack depth (a_o = 88 mm) and the crack extension (da = 15 mm) that approximates the onset of unstable ductile tearing. Points of tangency

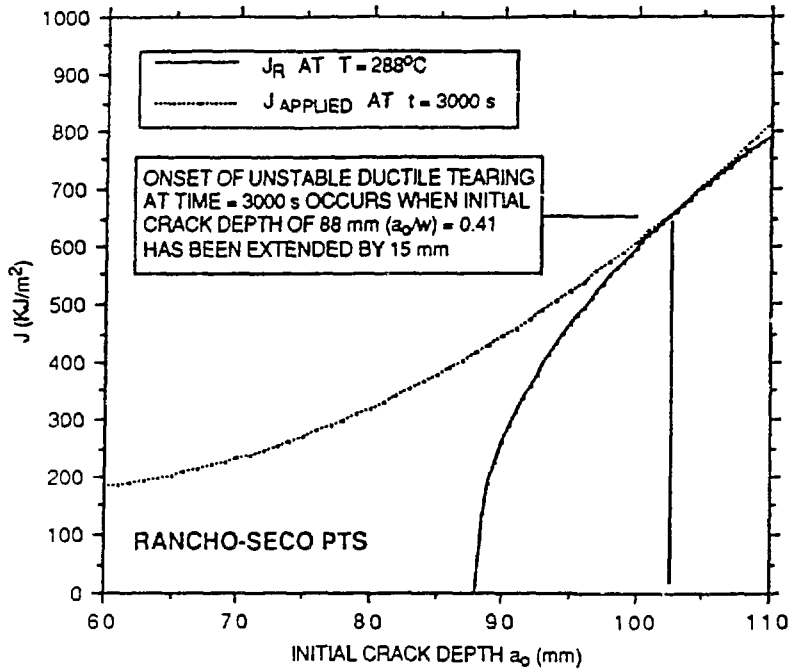

Fig. 4. Point of tangency defining initial crack depth and crack extension that approximates onset of unstable ductile tearing.

are obtained for various times throughout the transient to obtain a locus of points on the critical crack-depth plot corresponding to the onset of unstable ductile tearing.

The onset of unstable ductile tearing using the above methodology was found to be ~ 370 MPa • $\sqrt{m}$ for A533 B steel and ~240 MPa • $\sqrt{m}$ for low upper-shelf weld materials. More details of this ductile tearing analysis and results can be found in Ref. 18.

Influence Curves on the Benefit of the Enhanced Crack-Arrest Toughness Curves

By way of illustration, the onset of unstable ductile-tearing curves is included in Figure 5 for the Rancho Seco transient evaluation previously described. In this case, the enhanced crack-arrest potential is negated by unstable ductile tearing. It is apparent that crack arrest for some range of crack depths will take place, but in each case the arrest will be followed immediately by unstable ductile tearing to failure. For another range of flaw depths, no crack arrest takes place, resulting in failure by cleavage.

In general, the relative position of the critical crack-depth arrest curve and the unstable ductile-tearing curve are transient dependent. It appears that for higher pressure transients the enhanced crack-arrest potential will largely be negated by the inclusion of unstable tearing. However, for a lower pressure transient, the critical crack-depth arrest curve could cover the cleavage-initiation window at flaw depths less than those corresponding to the onset of unstable ductile tearing, thus preventing failure.

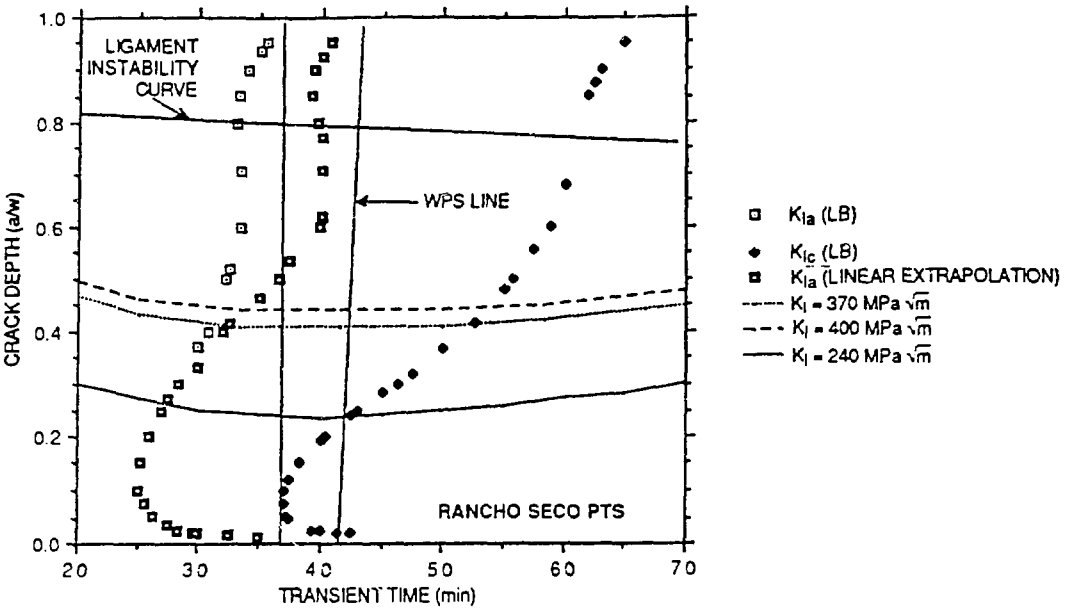

Fig. 5. Negation of enhanced crack-arrest potential by onset of unstable ductile tearing.

Effect of Enhanced K_C Data for Shallow Flaws on Deterministic Fracture Analysis

It is anticipated that A533 will show an increased fracture-initiation toughness associated with shallow flaws similar to that observed in the University of Kansas [9, 10] investigations for A36 and A517 for two primary reasons. First, the root cause of the shallow-crack toughness enhancement appears to be the loss of constraint at the crack tip for shallow cracks which is geometry dependent. Second, the stress-strain properties of A533 are bounded by those of A36 and A517 which have already been shown to exhibit an elevated toughness associated with shallow flaws. Furthermore, temperatures of interest in PTS analyses are both on the lower shelf and in the lower-transition region of the A533- material toughness curve. OCA-P is based on LEFM principles but has been used successfully at temperatures above the lower-shelf region. The enhanced initiation-fracture toughness due to shallow flaws does not qualify as "plane strain" fracture toughness. As a result, the critical-initiation toughness with the shallow-crack toughness elevation will hereafter be referred to as K_C instead of K_{IC}.

The University of Kansas shallow-crack investigations were conducted on laboratory sized, 3-point bend specimens using A36 (low strength, high-strain hardening) and A517 (high-strength, low-strain hardening) steels. Elevations in the initiation toughness measured in terms of Crack Tip Opening Displacement (CTOD) were shown at temperatures in the transition region of the steels rather than on the lower shelf. The shallow-crack fracture toughness was found to be about 2.5 times the conventional toughness for the A36 specimens and as high as four times the conventional toughness for the A517 specimens. The crack depths examined in the investigations which showed the elevated toughnesses were a = 4.8 mm (a/w = 0.15) for the A36 specimens and a = 3.8 mm (a/w = 0.15) for the A517 specimens. The crack depth in the deep-notched specimens (a/w = 0.50) were 15.9 and 12.7 mm for the A36 and A517 specimens, respectively.

To determine the impact of enhanced toughness for shallow flaws in PTS analyses, the toughness elevation of A533 material is estimated from available A36 and A517 data. In these specimens, the mechanism for the shallow-crack toughness elevation is due to a loss of constraint at the tip of the crack brought about by the close proximity of the crack tip to the free surface. However, as the specimen depth and the crack depth increase, it is believed that the toughness elevation will depend more on absolute crack depth (a) rather than normalized crack depth (a/w). The influence of a and a/w on the enhanced initiation toughness is currently under investigation for reactor pressure vessels. Therefore, the shallow-flaw initiation toughness increase estimates in this study are assumed to be a function of absolute crack depth rather than normalized crack depth. This assumption is conservative in that axial flaws up to 25 mm deep in a vessel wall nominally 200 mm thick could be considered "shallow" since the a/w ratio for these flaws is the same as tested at the University of Kansas [9, 10]. It was further assumed that no shallow-crack elevation takes place for cracks greater than 15.9 mm deep and that the toughness increases as the crack depth decreases but remains bounded as the crack depth approaches zero.

The fracture-initiation toughness enhancement is expressed in terms of an SC-factor which elevates the critical toughness for shallow flaws (K_C = SC-factor*ASME lower- bound curve). The CTOD data were converted to KJ_C values using the relationship found in Ref. 9. The SC-factor is related to the relative temperature ($T\text{-}RT_{NDT}$) and the maximum shallow-crack toughness increase, $(SC)_{max}$, which is based on the crack depth. In this way, the SC-factor is a function of both the temperature and crack depth.

The shallow-crack toughness enhancement (SC-factor) at a crack depth of 3.8 mm for A533 in the transition region is interpolated from the average A36 and A517 toughness increase based on the yield strength of the respective steels. The SC-factor for A36 specimens is increased by a small amount (3%) to account for the difference in crack depth between the A36 and A517 specimens. As described in Fig. 6, the SC-factor is assumed to be unity on the lower shelf which is up to

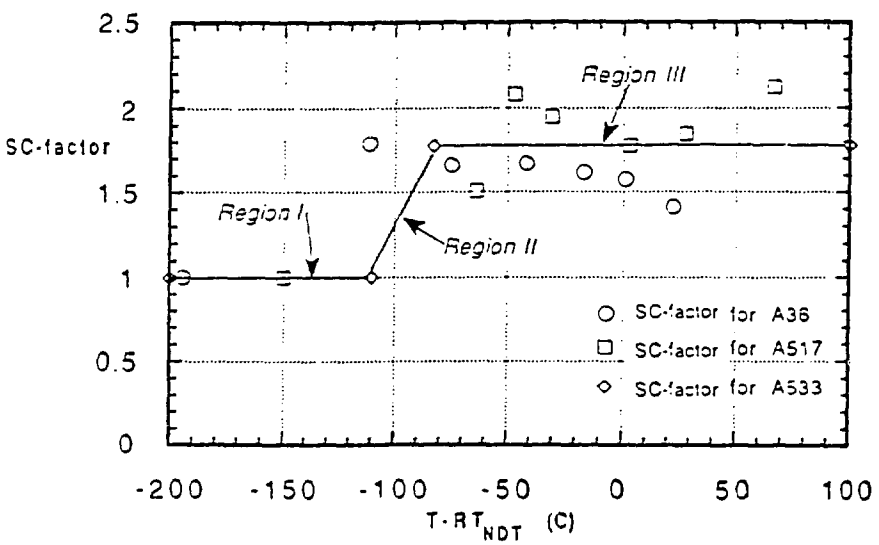

Fig. 6. The SC-factor for A533 was estimated using the A36 and A517 data for a = 3.8 mm and is divided into three regions.

about -110°C for A533 (Region I). The SC-factor is constant at $(SC)_{max}$ through the majority of the lower transition region of the toughness curve beginning at $T\text{-}RT_{NDT}$ of -83°C (Region III). In the region between the lower shelf and the lower-transition region, it is assumed that the SC-factor varies linearly with $T\text{-}RT_{NDT}$ (Region II). Fig. 6 shows the A36 and A517 data and the estimated SC-factor as a function of $T\text{-}RT_{NDT}$ for a crack depth of a = 3.8 mm showing the three regions.

The shallow-crack toughness enhancement as a function of crack depth, $(SC)_{max}$, is estimated for A533 using the two points based on the data from the University of Kansas [a = 3.8 mm, $(SC)_{max}$ = 1.78; a = 15.9 mm, $(SC)_{max}$ = 1.0]. Two different functions are used to describe the relationship between enhanced toughness and crack depth in order to determine the sensitivity of the probabilistic results to the shallow-crack enhancement and reflect the uncertainty of estimating the enhanced toughness prior to the collection of experimental data. The first function is simply a linear fit between the two data points with no shallow crack increase at crack depths greater than 15.9 mm. The second function is nonlinear and meets the additional constraint that the slope of the curve vanish at a crack depth of 15.9 mm. Both of these curves, shown in Fig. 7, remain bounded as the crack depth approaches zero. The general shape of both curves is similar to an enhanced toughness curve determined for a structural steel used in China [19].

The equations derived for the SC-factor are as follows:

Region I

SC-factor = 1.0 for $T\text{-}RT_{NDT} < -110°C$

Region II

SC-factor = $[(SC)_{max} - 1.0] / 27 * (T - RT_{NDT}) + 4.07 * (SC)_{max} - 3.07$

for $-110 < T\text{-}RT_{NDT} < -83°C$

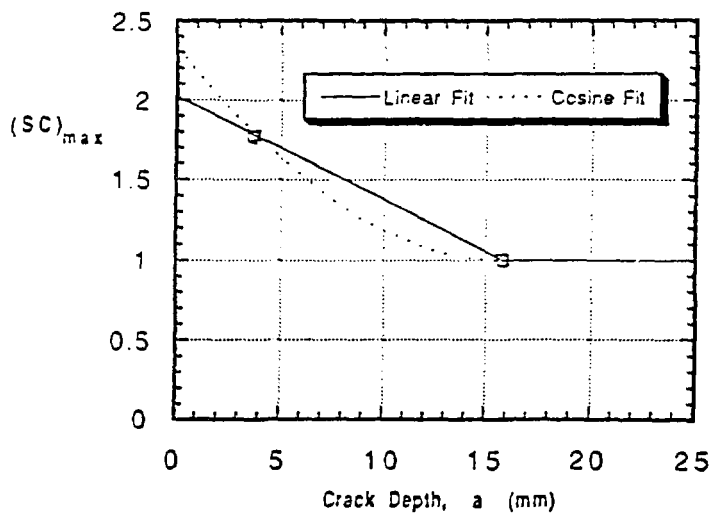

Fig. 7. $(SC)_{max}$ vs crack depth was determined using a linear and nonlinear fit from the two data points.

Region III
SC-factor = $(SC)_{max}$ for T-RT_{NDT} > -83°C.

$(SC)_{max}$ is determined both linearly or with a cosine fit as follows:

Linear Fit
$(SC)_{max}$ = 2.03 - 0.0645(a) for a <= 15.9 mm

Nonlinear Fit
$(SC)_{max}$ = 8.046 - 7.046 cos [(a/25.4) - 0.626] for a <= 15.9 mm.

$(SC)_{max}$ = 1.0 for a > 15.9 mm in both cases.

As an example of the estimated shallow-crack enhancement, Fig. 8 shows the ASME lower-bound curve and the shallow-crack enhanced toughness curve for a crack depth of 6.4 mm using the linear construction. For temperatures within the transition region, the toughness is increased over the lower-bound curve by a factor of 1.62. The impact of the enhancement is further illustrated in Fig. 9a which shows the critical crack depth curves at shallow-crack depths which corresponds to the ASME lower-bound curve and those resulting from the shallow-crack enhanced initiation toughness assuming both the linear and nonlinear formulations. The enhanced initiation toughness for shallow flaws increases the critical-flaw depths.

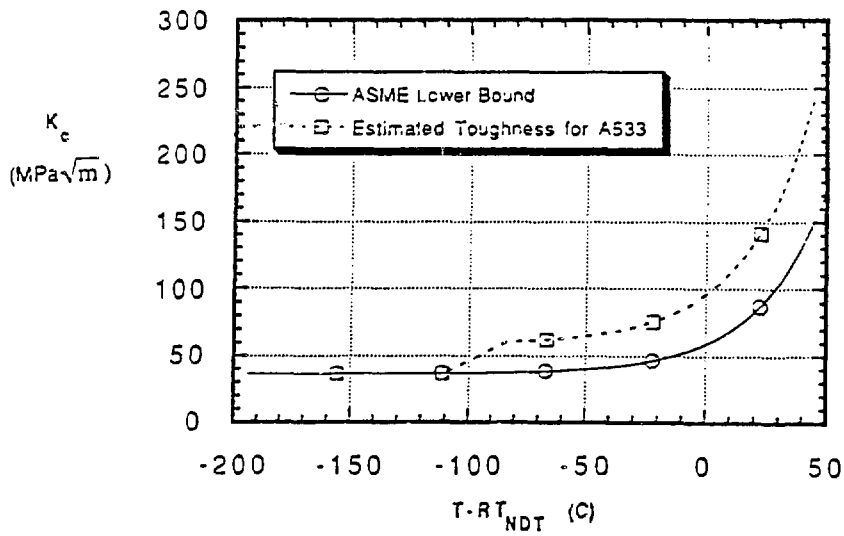

Fig. 8. Estimated toughness curve (linear fit) for A533 at a = 6.4 mm is compared with ASME lower-bound curve.

Probabilistic Considerations:

A probabilistic approach to the PTS issue, as developed in the IPTS studies and as required for compliance with Regulatory Guide 1.154, includes (1) the postulation of PTS transients, (2) an

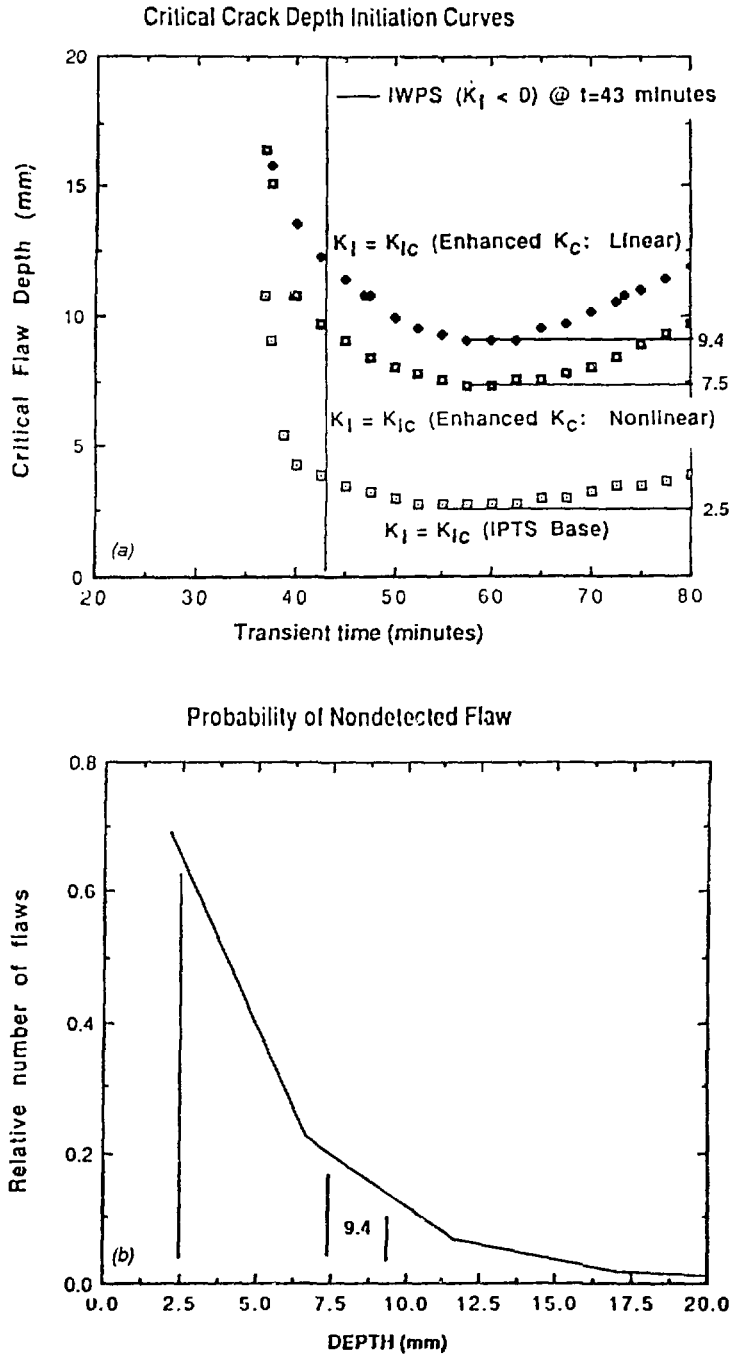

Fig. 9. Enhanced fracture toughness for shallow flaws increases the critical flaw depths and thus reduces the number of flaws of critical size.

Probabilistic Considerations:

A probabilistic approach to the PTS issue, as developed in the IPTS studies and as required for compliance with Regulatory Guide 1.154, includes (1) the postulation of PTS transients, (2) an estimation of their frequency of occurrence, (3) a systems analysis to determine the primary-system pressure, downcomer-coolant temperature and fluid-film heat-transfer coefficient on the inner surface of the vessel, and (4) a probabilistic fracture mechanics (PFM) analysis that uses the information from Item 3 as input. The PFM analysis provides an estimate of the conditional probability of failure, P(F|E), for each postulated transient. This is multiplied by the frequency of occurrence of the corresponding transient $\phi(E)$ and the product summed overall postulated transients to obtain the total frequency of failure $\phi(F)$ for a specific plant:

$$\phi(F) = \Sigma\, \phi_n(E)\, P_n\,(F|E)$$

where:

$\phi(F)$ = Total frequency of failure (failures per reactor year) for a specific plant

$\phi_n(E)$ = Frequency of occurrence of the n^{th} postulated transient (transient per year)

$P_n\,(F|E)$ = Conditional probability of failure of the n^{th} postulated transient (failures per transient), i.e., the probability of failure assuming that the transient does occur.

The individual products $\phi_n(E)P_n(F|E)$ define the order of dominance, i.e., they indicate the extent to which a particular transient contributes to the total frequency of failure for a specific plant [8]. In the IPTS studies, it was determined that the distinguishing characteristic of the dominant transients was high pressure. For the enhanced fracture- toughness data to significantly impact the total frequency of failure, it must reduce the conditional probability of failure for high-pressure dominant transients. The Rancho Seco transient is a high-pressure dominant transient and is chosen for evaluating the potential impact of the enhanced fracture-toughnes data on the conditional probability of failure relative to the probability corresponding to the fracture-toughness data bases utilized in the IPTS studies (referred to as the IPTS base case below).

The probabilistic distribution parameters utilized in all of the PFM analyses presented below were identical to those utilized in the IPTS studies and are the default values recommended by OCA-P [16].

Effect of Enhanced K_{Ia} on Results of PFM Analyses

In the IPTS study, a mean K_{Ia} curve of 1.25*K_{IR} (where K_{IR} is the ASME lower-bound K_{Ia} curve) was used and the onset of unstable ductile tearing was assumed to occur at 220 MPa • $\sqrt{m}$ [8]. The statistical mean curve for the combined large- and small-specimen HSST data base is shown in Fig. 10 to be steeper than the IPTS mean K_{Ia} curve. The statistical mean curve for the combined HSST large- and small-specimen data base can be expressed in terms of the IPTS K_{Ia}-mean curve with a correction factor as follows [18]:

$$(K_{Ia})_{mean}=1.25 * \{29.5 + 1.344 \exp [SAF * 0.0261 * (T-RT_{NDT}) + 89]\}$$

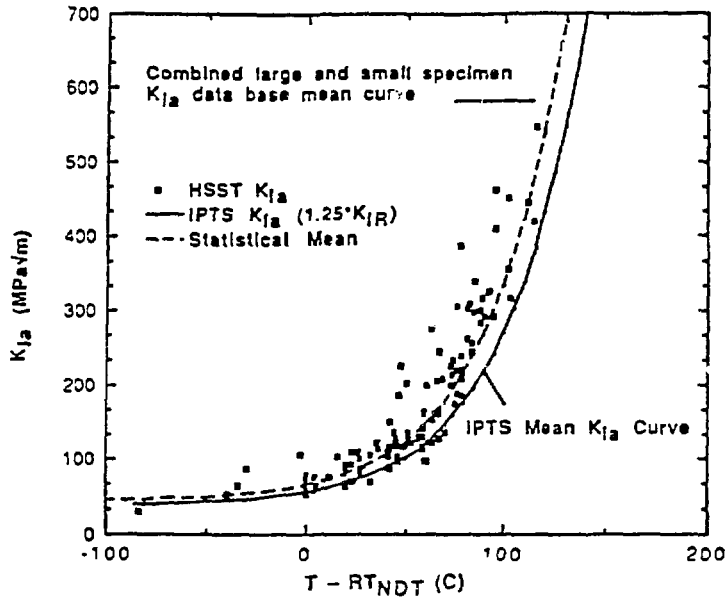

Fig. 10. The statistical mean curve for the combined HSST data base is steeper than the mean curve used in the IPTS study.

This correction factor was incorporated into OCA-P to examine the influence of the steeper mean K_{Ia} curve on the conditional probability of failure relative to the value calculated using the IPTS base case. Also, crack arrest is allowed to occur up to 370 MPa • $\sqrt{m}$ which is the approximation for the onset of unstable ductile tearing for nonLUSW materials discussed earlier.

The effect of the enhanced K_{Ia} data does reduce the conditional probability of failure; however, the reference is not significant. As illustrated in Table 1, P(FIE) decreases from .021 to .019.

Table 1. Summary of Probabilistic Fracture Mechanics Analysis of Rancho Seco PTS

Case	P(FIE)	$P(FIE)_{WPS}$	$\frac{P(FIE)_{WPS}}{P(FIE)}$	% Failures Due to Reinitiations
Base (IPTS PFM Model)	2.1 E-2	4.4 E-3	.21	0.2%
Enhanced K_{Ia}	1.9 E-2	3.1 E-3	.16	6.0%
Enhanced K_c (Linear K_c-Crack Depth)	3.2 E-3	6.0 E-4	.19	.03%
Enhanced K_c (Nonlinear K_c-Crack Depth)	5.5 E-3	1.1 E-3	.20	0%

P(FIE) – Calculated Conditional Probability of Vessel Failure without Including Type I Warm Prestress

$P(FIE)_{WPS}$ – Calculated Conditional Probablity of Vessel Failure Including Type I Warm Prestress

A noticeable effect of the enhanced K_{Ia} data is to shift the failures to a later time in the transient. This is illustrated in the histograms in Fig. 11. When the inhibiting effect of Type I warm prestress is included in the analysis, the effect of the enhanced K_{Ia} data becomes more significant. Approximately 82% and 86% of the failures occur after WPS for the IPTS base case and enhanced K_{Ia} case, respectively. A larger percentage of the total failures are due to cleavage reinitiations (6% for the enhanced K_{Ia} case compared to 0.2% for the IPTS base case).

Effect of Shallow Flaw Enhanced K_C on Results of PFM Analyses

It is anticipated that A533B, a prototypical nuclear reactor pressure vessel steel, will exhibit elevated (relative to the ASME K_{IC} curve) fracture-initiation toughness for shallow flaws. In the IPTS (base case) study, a mean K_{IC} curve of 1.43* K_{IC} (where K_{IC} is the lower-bound ASME fracture-initiation toughness curve) was utilized. To evaluate the potential impact of enhanced fracture-initiation toughness data on the conditional probability of failure, the IPTS mean K_{IC} was modified to simulate the shallow-flaw effect as follows:

$$(K_{IC})\ \text{mean} = (\text{SC-factor})*1.43*\text{ASME lower-bound } K_{IC} \text{ curve}$$

where the SC-factors as derived earlier were incorporated into OCA-P.

It is difficult to quantify the relation between enhanced fracture-initiation toughness and crack depth since only two data points are available. However, by utilizing both the linear and nonlinear functions derived earlier in the paper (Fig. 7), it is possible to determine the sensitivity and potential significance of the shallow-flaw effect on the results of PFM analyses. The linear relation is more optimistic whereas the nonlinear relation is probably more realistic because the slope of the $(SC)_{max}$ vs. a curve vanishes at a crack depth of 15.9 mm which is consistent with experimental observation

In both cases, the effect of the enhanced fracture-initiation toughness data does appear to significantly reduce P(FIE) relative to the original IPTS base case. As illustrated in Table 1, P(FIE) was reduced by nearly an order of magnitude (from .02 to .003) and by a factor of nearly 4 (from .02 to .005) for the linear- and nonlinear-K_C crack-depth relations, respectively. The potential significance and sensitivity of these results provides motivation for the HSST Program to verify and accurately quantify the shallow-flaw effect for future application to the PTS issue.

The critical crack-depth curves in Fig. 9a (which is similar to Fig. 3 except that Fig. 9a is restricted to shallow depths for clarity) illustrate how the enhanced K_C for shallow flaws increases the critical flaw depths, i.e., flaw depths for which $K_I=K_C$. The minimum critical flaw depths are approximately 2.5 mm, 7.6 mm, and 9.4 mm, corresponding to the IPTS base case, nonlinearly enhanced K_{IC}, and linearly enhanced K_C, respectively. The Marshall flaw-depth distribution function, used in OCA-P [16] and illustrated in Fig. 9b, defines the relative number of undetected flaws as a function of crack depth. Fig. 9b illustrates that increasing the critical flaw depths effectively reduces the relative number of flaws of critical size, thus reducing the conditional probability of failure.

The histograms in Fig. 12 illustrate results of PFM analyses for the IPTS base case and the nonlinearly enhanced K_C for the Rancho Seco PTS event. As illustrated, the crack depths at which initiation occurred were increased to depths for which the corresponding probability of having an undetected flaw is significantly reduced. The required number of vessels simulated to induce

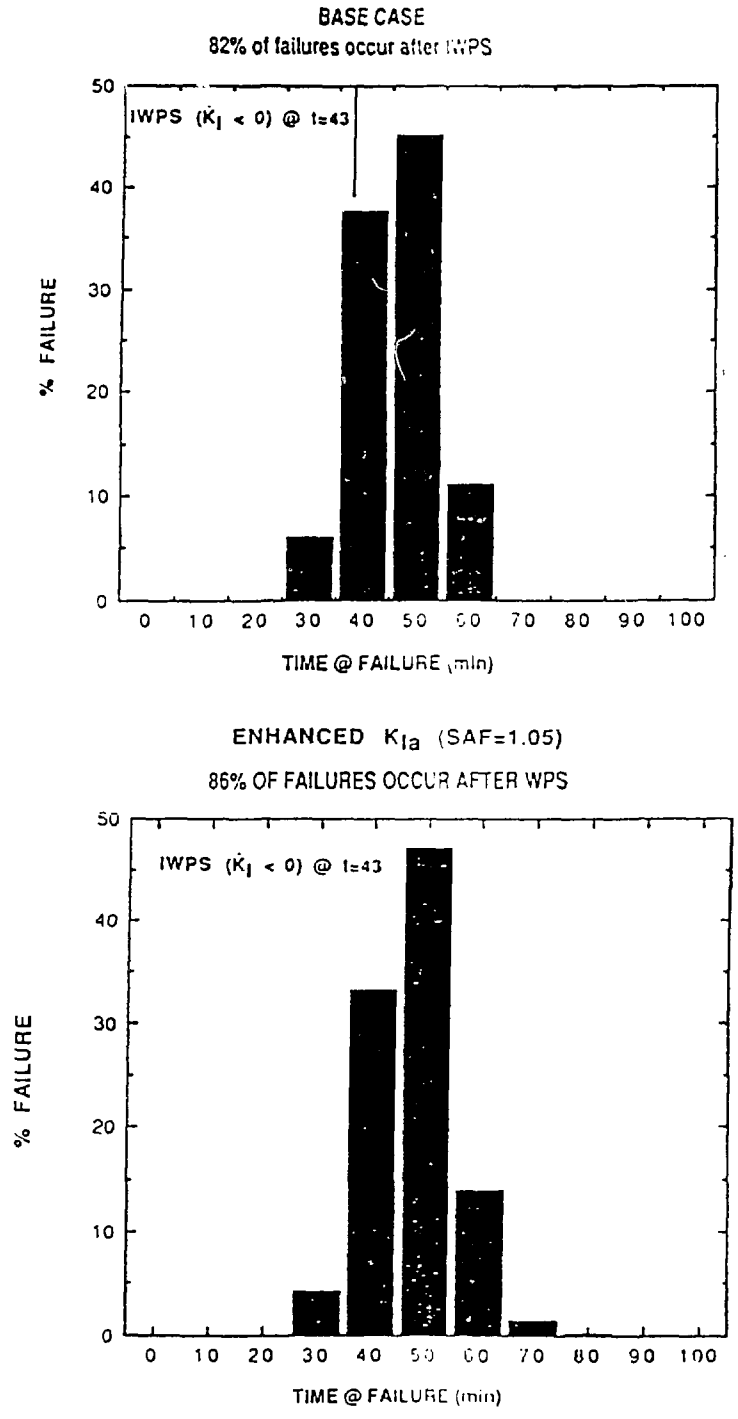

Fig. 11. Enhanced K_{Ia} data shifts failures to a later transient time thus benefiting more from Type-1 WPS.

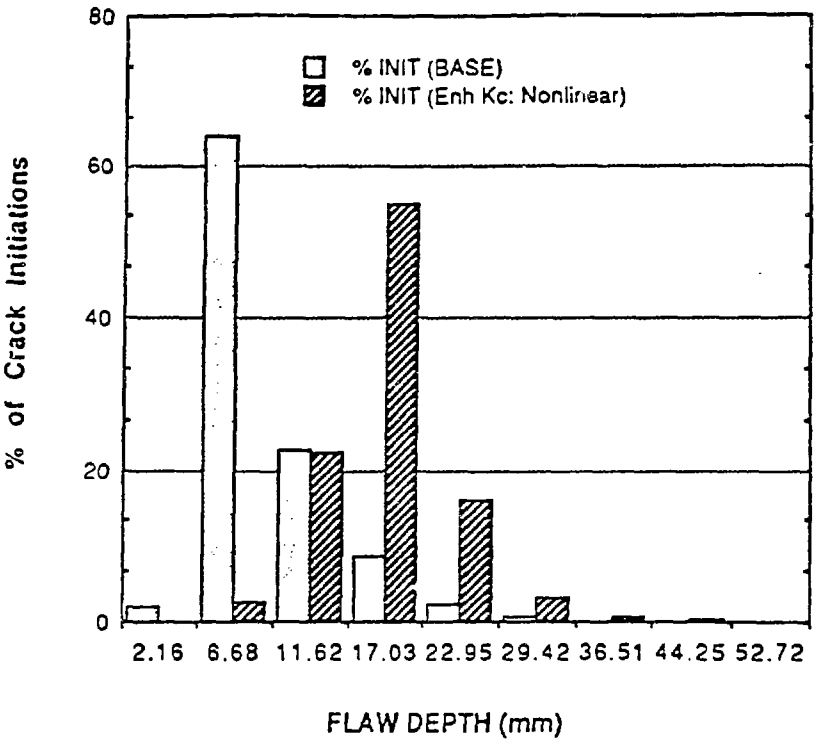

Fig. 12. Enhanced K_C data significantly reduces P(F/E) for two reasons: a) for shallow flaws, probability of crack initiation is reduced, and b) flaw density for critical size flaws is reduced.

approximately 3100 failures were 180000 for the IPTS base case and 720000 and the nonlinearly-enhanced K_C data, respectively.

Inclusion of Type I Warm Prestress on Results of PFM Analyses

Warm prestressing (WPS) has been recognized as an important physical phenomenon which can prevent the occurrence of cleavage fracture under certain conditions. The basic premise of Type I WPS, that a crack tip must have increasing plastic strain to propagate, was successfully demonstrated in the HSST Thermal Shock Experiments and Pressurized Thermal Shock Experiments [12, 13, 15].

The sensitivity of P(F|E) to the inhibiting effects of Type I WPS was considered in the original IPTS study; however, the effects were not included in the results. The IPTS study concluded that the benefit of Type I WPS is transient dependent and in some cases can be quite significant. The primary reasons that Type I WPS was not included in the original IPTS is that the K_I vs. time curves are relatively flat for the critical (shallow) flaws, making it difficult to identify the time at which $\dot{K}_I = 0$. Also, this time is quite sensitive to slight variations in the postulated transient and each transient calculated in detail represents a category of transients. Therefore, the time during the transient at which Type I WPS is effective is uncertain. For these reasons, Regulatory Guide 1.154 presently states that the inhibiting effect of WPS should not be assumed.

Incipient warm prestress occurs at approximately 43 minutes for the Rancho Seco PTS. As can be seen from Table 1, inclusion of WPS significantly reduces P(FIE). A methodology for including the beneficial effects of Type I WPS in IPTS type PFM analyses is currently under review.

CONCLUSIONS

Deterministic fracture-mechanics analyses have demonstrated that the application of the enhanced K_{Ia} data increases the probability of crack arrest; however, it appears that this potential benefit will be somewhat negated by the inclusion of unstable ductile tearing, particularly for the case of high-pressure, "dominant" transients. Probabilistic fracture- mechanics analyses have demonstrated that the application of the enhanced K_{Ia} data reduces the calculated probability of failure, but it is not by a significant margin for dominant transients. The benefit of the enhanced K_{Ia} data is more significant when the inhibiting effect of Type I warm prestress is included in the model.

Deterministic fracture mechanics analyses have demonstrated that the application of enhanced K_c data for shallow flaws eliminates crack initiation for a range of shallow-flaw depths. Probabilistic fracture-mechanics analyses have demonstrated that the application of the enhanced K_c data significantly reduces the calculated probability of failure. The potential significance and sensitivity of these results provides motivation for the HSST program to verify and more accurately quantify the shallow-flaw effect for future application to the PTS issue.

The effect of the shallow-crack enhanced fracture-toughness data on PTS analyses is transient dependent and also dependent on the flaw-size distribution; therefore, it is difficult to quantify with precision the effect of the enhanced fracture-toughness data until probabilistic fracture-mechanics analyses have been performed that will consider a wide variety of postulated transients for a specific plant. It can be safely assumed that the application of the enhanced fracture-toughness data will result in a reduced probability of vessel failure relative to the model utilized in the original IPTS.

References

1. R. D. Cheverton, S. K. Iskander, and D. G. Ball, Union Carbide Corp., Nuclear Div., Oak Ridge Natl. Lab., *PWR Pressure Vessel Integrity During Overcooling Accidents: A Parametric Analysis*, USNRC Report NUREG/CR-2895 (ORNL/TM-7931, February 1983.

2. R. D. Cheverton and D. G. Ball, Martin Marietta Energy Systems, Inc., Oak Ridge Natl. Lab., "Probabilistic Fracture Mechanics Analysis of Potential Overcooling Sequences," pp. 263-306 in *Pressurized-Thermal-Shock Evaluation of the H. B. Robinson Nuclear Power Plant*, USNRC Report NUREG/CR-4183, Vol. 1 (ORNL/TM-9567/V1), September 1985.

3. R. D. Cheverton and D. G. Ball, Martin Marietta Energy Systems, Inc., Oak Ridge Natl. Lab., *Pressurized-Thermal-Shock Evaluation of the Calvert Cliffs Unit 1 Nuclear Power Plant*, USNRC Report NUREG/CR-4022 (ORNL/TM-9408), September 1985.

4. R. D. Cheverton and D. G. Ball, Martin Marietta Energy Systems, Inc., Oak Ridge Natl. Lab., *Preliminary Development of an Integrated Approach to the Evaluation of Pressurized-Thermal-Shock as Applied to the Oconee Unit 1 Nuclear Power Plant*, USNRC Report NUREG/CR-3770 (ORNL/TM-9176), May 1986.

5. *Code of Federal Regulations*, Title 10, Part 50, Section 50.61 and Appendix G.

6. U.S. Nuclear Regulatory Commission, Regulatory Guide 1.154, "Format and Content of Plant-Specific Pressurized Thermal Shock Safety Analysis Reports for Pressurized Water Reactors."

7. *The American Society of Mechanical Engineers Boiler and Pressure Vessel Code*, Section XI, Rules for Inservice Inspection of Nuclear Power Plant Components, 1986.

8. R. D. Cheverton and D. G. Ball, "Application of Probabilistic Fracture Mechanics to the Pressurized-Thermal-Shock Issue," pp. 35-50 in *Fracture Mechanics: Eighteenth Symposium, American Society for Testing and Materials*, ASTM STP 945, Philadelphia, 1988.

9. W. A. Sorem, Exxon Corp., R. H. Dodds, Jr., Univ. of Ill., and S. T. Rolfe, Univ. of Kansas, *An Analytical Comparison of Short Crack and Deep Crack CTOD Fracture Specimens of an A36 Steel; The Effects of Crack Depth on Elastic Plastic CTOD Fracture Toughness; A Comparison of the J-Integral and CTOD Parameters for Short Crack Specimen Testing*, Welding Research Council Bulletin 351, February 1990.

10. J. A Smith, Butler Manufacturing Co., and S. T. Rolfe, Univ. of Kansas, *The Effect of Crack Depth to Width Ratio on the Elastic-Plastic Fracture Toughness of a High-Strength, Low-Strain Hardening Steel*, February 1990.

11. T. J. Theiss, Martin Marietta Energy Systems, Inc., Oak Ridge Natl. Lab., *Recommendations for the Shallow-Crack Fracture Toughness Testing Task Within the HSST Program*, USNRC Report NUREG/CR-5554 (ORNL/TM-11509),October 1990.

12. R. H. Bryan et al., Martin Marietta Energy Systems, Inc., Oak Ridge Natl. Lab., *Pressurized-Thermal Shock Test of 6-in.-Thick Pressure Vessels. PTSE-1: Investigation of Warm-Prestressing and Upper-Shelf Arrest*, USNRC Report NUREG/CR-4106 (ORNL-6135), 1987.

13. R. H. Bryan et al., Martin Marietta Energy Systems, Inc., Oak Ridge Natl. Lab., *Pressurized-Thermal Shock Test of 6-in.-Thick Pressure Vessels. PTSE-2: Investigation of Low Tearing Resistance and Warm Prestressing*, USNRC Report NUREG/CR-4888 (ORNL-6377), 1987.

14. D. J. Naus, J. Keeney-Walker, and B. R. Bass, "High Temperature Crack-Arrest Behavior of Prototypical and Degraded (Simulated) Reactor Pressure Vessel Steels," *Int. J. Pressure Vessels and Piping* 39, 1989.

15. R. D. Cheverton et al., Martin Marietta Energy Systems, Inc., Oak Ridge Natl. Lab., *Pressure Vessel Fracture Studies Pertaining to the PWR Thermal-Shock Issue: Experiments TSE-5, TSE-5A, and TSE-6*, NUREG/CR-4249 (ORNL-6163), June 1985.

16. R. D. Cheverton and D. G. Ball, Martin Marietta Energy Systems, Inc., Oak Ridge Natl. Lab., *OCA-P, A Deterministic and Probabilistic Fracture-Mechanics Code for Application to Pressure Vessels*, USNRC Report NUREG-3618 (ORNL-5991), May 1984.

17. L. B. Freund et al., *A Short Course on Advanced Topics in Fracture*, Brown University, Providence, Rhode Island, 1989.

18. T. L. Dickson et al., Martin Marietta Energy Systems, Inc., Oak Ridge Natl. Lab., *Inclusion of Unstable Ductile Tearing and Extrapolated Crack-Arrest Toughness Data in PWR Integrity Assessment* , USNRC Report NUREG/CR-5473 (ORNL/TM-11450), May 1990.

19. D. Z. Zhang and H. Wang, Harbin Shipbuilding Inst., "On the Effect of the Ratio a/w on the Values of d_i and J_i in a Structural Steel," *Engineering Fracture Mechanics*, Vol. 26, No. 2, pp. 247-250, 1987.